JOURNAL OF MATERIALS SCIENCE 24 (1989) 1729–1738

Crack growth in transforming ceramics under cyclic tensile loads

L. A. SYLVA, S. SURESH
Division of Engineering, Brown University, Providence, Rhode Island 02912, USA

The mechanisms of stable growth of short fatigue cracks (crack length up to 1 mm) at room temperature in magnesia-partially stabilized zirconia subjected to cyclic tensile loads were investigated. Single edge-notched specimens were fractured in the four-point bend configuration under cyclic and quasi-static tensile loads. At a load ratio of 0.1, the threshold stress intensity factor range, ΔK, for fracture initiation in cyclic tension is as low as 3.4 MPa $m^{1/2}$, and catastrophic failure occurs at ΔK = 6.6 MPa $m^{1/2}$. For crack length less than 1 mm and for plane strain conditions, growth rates are highly discontinuous, and periodic crack arrest is observed after growth over distances of the order of tens of micrometres. Crack advance could only be resumed with an increase in the far-field stress intensity range. The mechanisms of short crack advance in cyclic tension are similar to those observed under quasi-static loads, and the tensile fatigue effect appears to be a manifestation of "static failure modes". A model is presented to provide an overall framework for the tensile fatigue crack growth characteristics of partially stabilized zirconia. Experimental results are also described to demonstrate the possibility of stable room temperature crack growth under cyclic tension in fine-grained tetragonal zirconia polycrystals, partially stabilized with Y_2O_3. The growth of cracks in transformation-toughened ceramics is found to be strongly influenced by the crack size and shape, stress state and specimen geometry.

1. Introduction

The successful use of ceramic materials in potential structural applications requires a thorough understanding of their resistance to fracture under cyclic loads. Although substantial progress has recently been made in the theoretical and experimental studies of toughening mechanisms for brittle solids (e.g. [1]), the fatigue behaviour of ceramics has remained a relatively unexplored topic. This lack of knowledge is an outcome of the general notion that ceramic materials do not exhibit stable fatigue crack growth at room temperature due to the paucity of appreciable plastic deformation. The few limited sets of exploratory studies previously reported in the literature have provided only an ambiguous picture of the possible mechanical fatigue effects in brittle ceramics [2–6].

In a recent study, Ewart and Suresh [7, 8] demonstrated that the application of cyclic compressive stresses to notched plates of polycrystalline alumina could lead to stable Mode I fatigue crack growth at room temperature. This "metal-like" behaviour has since been found by Suresh and coworkers [9–13] in a wide range of ceramics and ceramic composites including hot-pressed Si_3N_4, metastable zirconia (ZrO_2 partially stablized with MgO or Y_2O_3), Al_2O_3 or Si_3N_4 ceramics reinforced by SiC whiskers, cemented carbides (WC–Co, TiC–Ni), and concrete. Detailed finite element analyses have shown that the principal mechanism for such Mode I fatigue crack growth is the generation of residual tensile stresses when the inelastic deformation at the notch-tip leaves permanent strains upon unloading from the far-field compressive stress [11]. This Mode I fracture phenomenon is an intrinsic mechanical fatigue effect in that it is observed only under far-field cyclic compressive stresses and that the mode of fracture is markedly different from that observed under static loading or in a corrosive environment.

The above work has also clearly established that toughening mechanisms which lead to improved strength and toughness combinations for brittle ceramics may, infact, give rise to inferior fatigue crack growth resistance. Furthermore, such results illustrate that in ceramics containing defects and stress concentrations, low nominal cyclic compressive stresses (even as low as one tenth of the compressive strength) can promote significant levels of subcritical crack growth at room temperature. Thus, the traditional notion that brittle materials are much safer in compression than in tension has to be re-evaluated in the context of cyclic compressive loads.

Although ceramic materials do not exhibit macroscopic plastic deformation at room temperature, one might anticipate some type of subcritical crack growth under cyclic tension in toughened ceramics due to their well-documented resistance curve behaviour in quasi-static tension. Indeed, it is now experimentally established that stress-induced martensitic transformation in metastable zirconia can be accompanied by up to a five-fold increase in fracture toughness of the PSZ in comparison to that of the fully stable ceramic microstructure [1, 14–16]. Continuum studies

0022–2461/89 $03.00 + .12

of stress-induced dilatant transformation show that, during crack growth, the residual strain fields associated with the transformed particles in the wake of the advancing crack front limit crack opening displacement and cause an increase in the apparent stress intensity factor for further fracture [17–19]. Constitutive models which consider both the volumetric and shear strains induced by transformation predict even a greater toughening effect than those indicated by the pure dilation-toughening models [12, 20].

Experimental studies of tensile–compressive fatigue in transforming ceramics by Swain and Zelizko [21] and by Bowen *et al.* [22] have indicated the possibility of a mechanical fatigue effect. Subsequent tensile fatigue experiments by Dauskardt *et al.* [23] show that crack growth can occur at stress intensity range values as low as $3\,MPa\,m^{1/2}$, well below the quasi-static toughness or the threshold for stress corrosion cracking. Significant crack closure was also detected in the near-threshold regime of fracture where the growth rates were highly sensitive to the mean stress of the fatigue cycle. Although the existence of subcritical crack growth under cyclic compression and cyclic tension in transforming ceramics is now evident, the mechanisms underlying such effects are largely unknown.

The objective of the present work was to investigate the salient features and mechanisms of subcritical crack growth in 9 mol % MgO-PSZ subjected to fully tensile loads at room temperature using four-point bend specimens. The rate of fatigue crack advance, from the threshold for crack growth to final fracture, was monitored through optical microscopy. The threshold stress intensity range for the growth of through-thickness short cracks (length up to 1 mm) was about $3.4\,MPa\,m^{1/2}$ at a load ratio $R = 0.1$. However, as a result of crack arrest induced by closure of the crack faces in the transformed wake of the advancing crack front, sub-critical crack growth was found to be highly discontinuous in nature. Further crack growth could only be re-initiated with an increase in the applied stress intensity factor range. The self-arrest of cracks in zirconia has also been found in notched specimens subject to a static tensile load. These results indicate that the threshold for crack growth in cyclic tension occurs when the maximum stress intensity factor of the fatigue cycle exceeds the quasi-static toughness of the fully stabilized zirconia. Similarly, catastrophic final fracture is observed when the maximum stress intensity factor exceeds the steady state toughness value (determined from the resistance curve) for the partially stabilized zirconia. The occurrence of such "quasi-static" failure modes during cyclic tension is also supported by a variety of experimental observations. A model is presented in an attempt to rationalize the experimentally observed tensile fatigue crack growth behaviour of partially stabilized zirconia ceramic. In addition to the results reported for Mg-PSZ, it is demonstrated that it is possible to obtain stable Mode I crack growth under tension–tension fatigue in tetragonal zirconia polycrystals, partially stabilized with Y_2O_3.

2. Materials and experimental procedures

2.1. Materials

Crack growth under cyclic tension was investigated primarily in a MgO-partially stabilized zirconia (Mg-PSZ). This material, characterized as MS-grade (maximum strength), was obtained from Nilcra Ceramics, Inc., St Charles, Illinois. It contains approximately 9 mol % MgO as a stabilizer in solid solution, 15 mol % fully stabilized cubic zirconia, as well as about 40 mol % metastable tetragonal phase. The microstructure consists of a cubic matrix with grains of approximately 50 μm diameter. Within this matrix are lens-shaped precipitates of the metastable tetragonal phase, about 300 nm in length. More detailed descriptions of the microstructure of this material can be found elsewhere [1, 14, 21]. The room-temperature mechanical properties of this grade of PSZ were quoted by the supplier as: compressive strength = 1850 MPa, flexural strength = 725 MPa, and Young's modulus = 205 GPa. In additon to the tests performed on Mg-PSZ, the possibility of stable fatigue crack growth in cyclic tension was explored in a zirconia ceramic partially stabilized with Y_2O_3.

2.2. Fatigue experiments

Single edge-notched specimens of Mg-PSZ were machined to the following dimensions: width $W =$ 10.1 mm, height $H = 50.8$ mm, thickness $B = 8.46$ mm, notch length-to-specimen width ratio $a/w = 0.36$, notch angle $\theta = 60°$, and notch-root radius $\varrho =$ 0.12 mm. The side surfaces of the specimens were first ground and polished with a diamond paste (grit size 1 μm) in order to make the formation of the crack more readily visible. Following the recent studies on cyclic compression fatigue [8, 13], a single cycle of compressive stress (maximum value = 383 MPa) was applied to the specimen to facilitate the nucleation of a fatigue crack at the notch-tip. Subsequently, the specimen was subjected to cyclic tension in four-point bending in an electro-servohydraulic machine. (Some experiments were also conducted without a fatigue pre-crack induced in cyclic compression.) Several tensile fatigue tests were conducted where the length of the Mode I crack was up to 1 mm. We note that this maximum tensile fatigue crack length is up to nine times the notch-root radius, ϱ, and therefore, the measured crack growth characteristics are expected to be free of the effects of notch-tip fields. For an elastic material, the strain field of the notch is known to affect the growth behaviour of a fatigue crack emanating from the notch-tip over a distance ahead of the notch of only 1/20 to 1/40 times the notch-root radius.

Crack growth was monitored, on both side surfaces of the specimen, with the aid of an optical microscope. Furthermore, the length of the arrested cracks was also measured in a high-resolution light microscope and in the scanning electron microscope. The constant amplitude cyclic tension experiments were conducted in a room-temperature laboratory environment (temperature $\approx 22°C$, relative humidity $\approx 40\%$) at a fixed cyclic frequency of 10 Hz and a load ratio of 0.1.

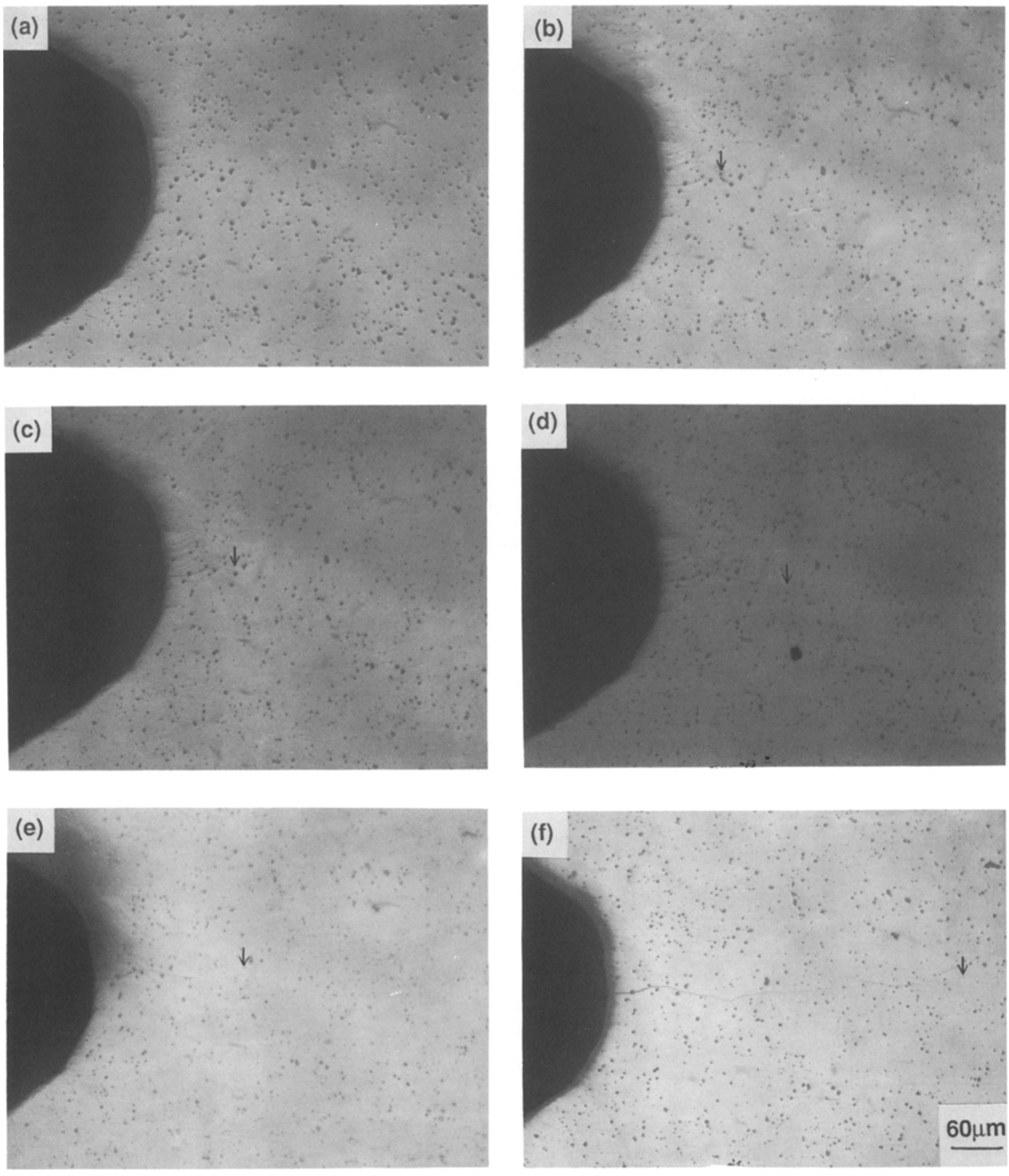

Figure 1 A series of optical micrographs showing the crack profile during the fatigue test: (a) notch-tip geometry prior to the fatigue test; (c to f) a pre-crack induced at the notch-tip after one compression cycle; (c to f) tensile fatigue cracks propagated at various ΔK levels: ΔK = (c) 3.52 (d) 4.5 (e) 4.9, and (f) 6.65 MPa $m^{1/2}$. The arrows indicate the crack-tip location.

Note that the load ratio, R, is defined as

$$R = \frac{K_{min}}{K_{max}} \tag{1a}$$

and the nominal stress intensity factor range is

$$\Delta K = K_{max} - K_{min} \tag{1b}$$

Where K_{min} amd K_{max} are the minimum and maximum stress intensity factors, respectively, during the fatigue cycle. The stress intensity factor, K, for the four-point bend geometry was calculated using the formula [24]

$$K = \frac{P}{B(W)^{1/2}}\left[5.96\left(\frac{a}{w}\right)^{1/2} - 7.39\left(\frac{a}{w}\right)^{3/2} + 38.92\left(\frac{a}{w}\right)^{5/2} - 69.66\left(\frac{a}{w}\right)^{7/2} + 74.44\left(\frac{a}{w}\right)^{9/2}\right] \tag{2}$$

The fatigue experiments were started at an initial stress intensity range, ΔK = 1 MPa $m^{1/2}$. If no

crack growth was detected over 100 000 cycles, the ΔK value was raised by 0.5 MPa $m^{1/2}$. This process was repeated until the threshold for crack growth was monitored at a constant value of the applied cyclic load and R ratio. If crack arrest occurred during the tension test, the loads (and hence ΔK) were raised in increments of no more than 0.3 MPa $m^{1/2}$ until the arrested crack could be reinitiated. The results of the above experiments were used to plot the variation of crack growth rates per cycle (da/dN) as a function of the nominal stress factor range, ΔK.

2.3. Fracture toughness measurements

In order to compare the crack growth behaviour under cyclic tensile loads with that observed under quasi-static tensile loads, the fracture toughness and R curve behaviour of the partially stabilized zirconia ceramic were also investigated. In this case, single edge-notched specimens of the same dimensions were pre-cracked in uniaxial cyclic compression at a constant compressive stress amplitude = 312 MPa and load ratio, $R = 10$, following the procedure outlined previously [13]. Cracks propagating along the plane of the notch progressively decelerate with an increase in the number of compression cycles and arrest completely. Upon crack arrest, the specimen was quasi-statically fractured in four-point bending with the crack on the tension side of the bend fixture. The applied load, which was recorded from the test machine, and the crack-mouth opening displacement, which was recorded from a clip gauge, were monitored to derive the critical stress intensity factor pertinent to the onset of catastrophic fracture, K_{Iss}. As the fatigue pre-crack develops a fully developed wake due to the hundreds of thousands of imposed compressive cycles, the onset of catastrophic fracture in this quasi-static experiment corresponds to the steady state value of the resistance curve.

2.4. Static load fracture experiments

As the mechanisms of crack growth in the cyclic tension tests were found to be similar to those observed under quasi-static loads, selected tests were also performed under static loads. If crack arrest occurred during a fatigue test, a slightly higher static tensile load was applied to the specimen to check (i) whether crack growth could be restarted and (ii) if, after a certain amount of growth under a static tensile load, the crack arrested naturally. The results of such interrupted static tests during some of the fatigue experiments were used in the interpretation of the mechanisms of fatigue failure.

3. Experimental results

3.1. Fatigue crack growth

Fig. 1 is a sequence of optical micrographs showing the crack length and morphology on one side of a notched specimen subjected to fatigue loads. Fig. 1a shows the notch geometry prior to the commencement of the experiments. The extent of the fatigue pre-crack emanating from the notch-tip due to the application of one cycle of compressive stress is evident in Fig. 1b.

TABLE I Results of stable fatigue crack growth at select ΔK levels

Nominal stress intensity range, ΔK (MPa $m^{1/2}$)	Stable crack growth distance prior to arrest, Δa^* (μm)
3.45	36.9
4.45	18.8
4.86	17.2
5.10	10.0
5.50	23.2

ΔK and Δa^* values reported here are based on the average of the crack length measurements from the two side surfaces. The ΔK values refer to the initial stress intensity range during each increment of crack growth.
The above results were obtained at a fixed R value of 0.1.

The changes in length of the tensile fatigue crack, as the applied ΔK increased from the threshold value to final fracture, is illustrated in the series of photographs provided in Figs 1c to 1f. These figures show that a macroscopically straight Mode I fatigue fracture is obtained in the tensile fatigue experiments. Fig. 2 exhibits the variation of the fatigue crack growth rate, da/dN, as a function nominal K_{max} and of the nominal stress intensity factor range, ΔK. Here, both the crack length and the stress intensity were calculated using the average values of crack length measured on the two side surfaces of the specimen. The maximum variation in total crack length between the two side surfaces was typically less than 6%. Note that, for the high-frequency fatigue test, the average da/dN values in Fig. 2 were calculated based on crack advance over thousands of load cycles, even though such fracture may have occurred during one cycle. Therefore, the da/dN values at different ΔK levels do not characterize cycle by cycle crack growth. Fig. 2 indicates that the threshold stress intensity factor range, ΔK_0, for crack growth in partially stabilized zirconia was approximately 3.4 MPa $m^{1/2}$. This value of threshold is comparable to that observed in recent cyclic tension experiments on Mg-PSZ [23]. A distinctly different fatigue behaviour revealed by the results shown in Fig. 2, however, is that the short tensile crack arrests completely after propagating a distance of between 10 to 36 μm, depending on the ΔK, level (see Table I). Because of this small distance of crack advance and the drastic fluctuations in the rates of crack propagation, the reported growth rates are subjected to some uncertainty. However, the arrest of the tensile fatigue crack at a constant amplitude of the far-field cyclic stress was confirmed by ensuring that no further fracture occurred for at least 100 000 cycles. Further growth of the arrested crack could not be obtained unless the far-field stress intensity factor was raised. This process was repeated until a ΔK value of about 6.6 MPa $m^{1/2}$ where catastrophic failure occurs. The fatigue experiments conducted on notched specimens containing no fatigue pre-cracks (induced by cyclic compression) also reveal discontinuous crack growth behaviour and final fracture ΔK similar to that described in Fig. 2. However, the threshold ΔK_0 values obtained in the four-point bend specimens without a pre-crack are not reliable due to the strong effect of the notch-tip geometry.

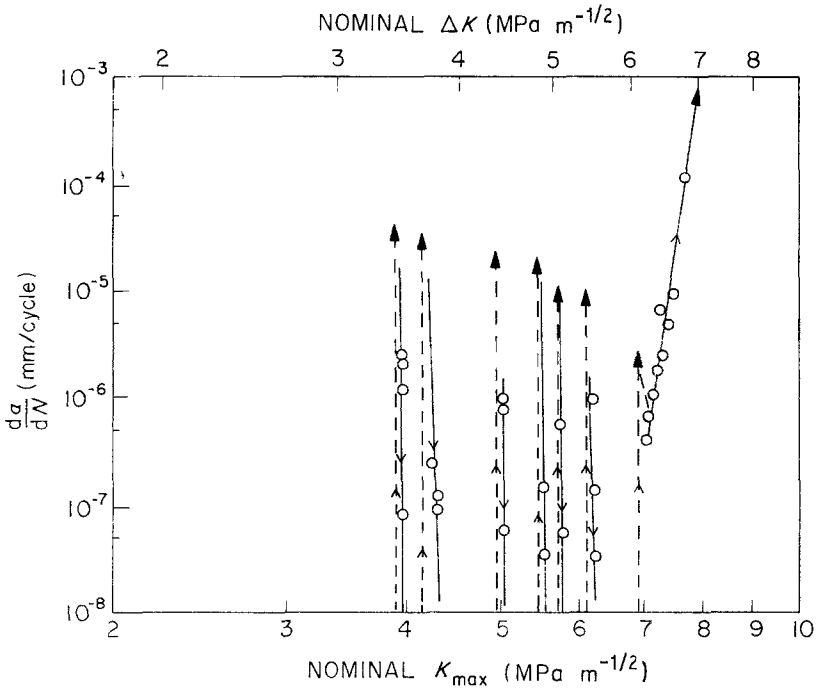

Figure 2 Fatigue crack growth rate, da/dN, plotted as a function of the applied stress intensity factor range. See text for details.

3.2. Static tensile fracture

In addition to cyclic tension loading, some specimens were subjected to static loads during the fatigue test in an attempt to compare the fatigue crack growth behaviour with any stable fracture that may occur during the application of the static load. For example, a fatigue crack was propagated in a notched zirconia specimen until crack arrest occurred at a ΔK value of about 3.8 MPa $m^{1/2}$. At this point, the specimen was subjected to a static load at an initial stress intensity factor value of 4.4 MPa $m^{1/2}$. The static load resulted in crack growth over a distance of approximately 15 μm; subsequently, the crack arrested completely. A similar effect was also observed at a static load corresponding to an initial stress intensity factor value of about 6 MPa $m^{1/2}$. These results show the similarities in the basic mechanisms of fracture under static and cyclic tensile loading conditions.

3.3. Quasi-static tensile fracture

The maximum critical stress intensity factor for catastrophic fracture initiation under quasi-static tensile loads was also estimated using fatigue-precracked single edge-notched specimens of Mg-PSZ fractured in four-point bending. The load at which catastrophic fracture occurred was used to calculate the steady state stress intensity factor, K_{Iss}, (in the K_I against crack extension curve or R curve). This stress intensity is an indication of the maximum fracture toughness that can be attained in a partially stabilized zirconia. Several such experiments were conducted and the average value of K_{Iss} was found to be about 7.5 MPa $m^{1/2}$ for the MS grade of Mg-PSZ.

3.4. Fractography

Fig. 3 shows scanning electron micrographs of the tensile fatigue fracture surface at different magnifications. Here the failure mode appears to be intergranular (Fig. 3a); at higher magnifications, some evidence of a transgranular mode of separation can also be seen. Fractographs showing the failure mode in quasi-static tensile fracture are provided in Fig. 4 at two different magnifications. However, comparison of Figs 3 and 4 reveals that the failure mechanisms are

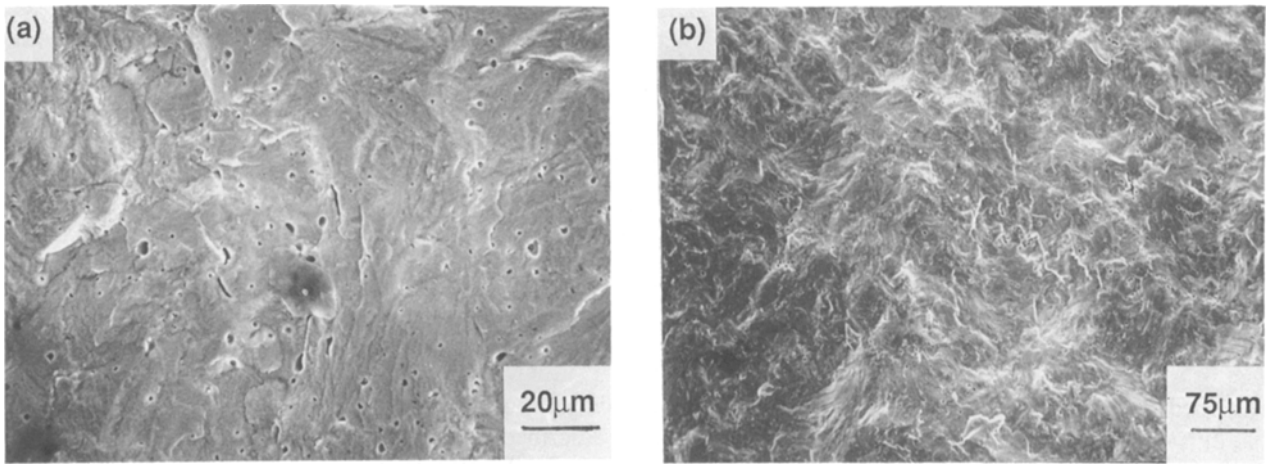

Figure 3 (a), (b) Scanning electron micrographs showing the fracture morphology during tension fatigue at different magnifications in ,g-PSZ; $\Delta K \approx 5$ MPa $m^{1/2}$.

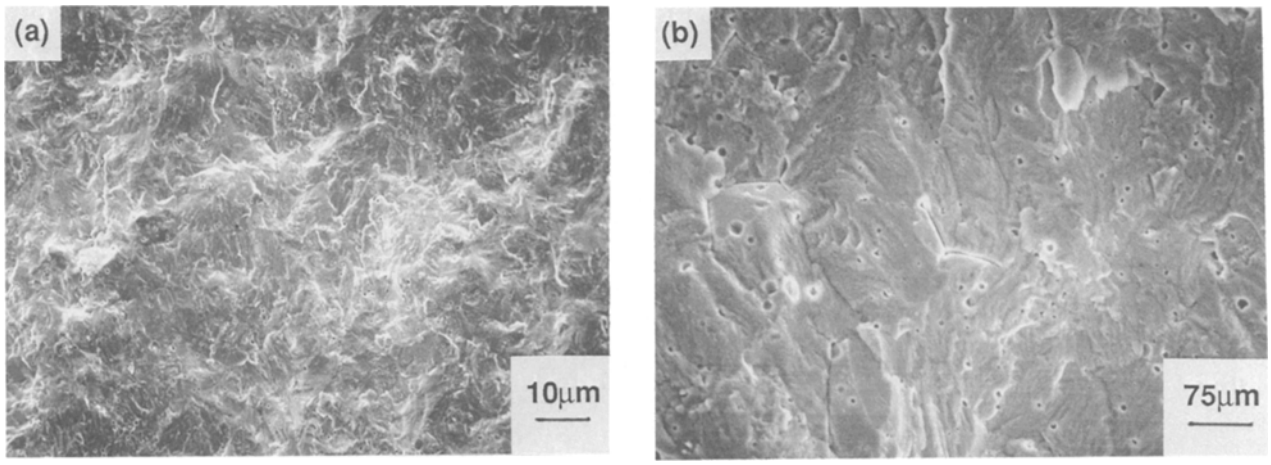

Figure 4 Fractography of quasi-static tensile failure at $K_I \approx 6.5 MPa\,m^{1/2}$.

similar in the quasi-static and cyclic tension experiments. The fracture morphology during cyclic compression failure appears to be somewhat different, as shown in Figs 5a and b, from experiments on two different Mg-PSZ specimens. In both Fig. 5a and b, considerable transgranular tearing can be noticed through the thickness of the specimens, with the local direction of failure of the fatigue pre-crack deviating away from the plane of the notch (although it is not readily obvious from one side view of the crack shown in Fig. 1a). This type of failure was also predicted by recent numerical analyses based on a constitutive model which incorporates the effects of both dilation and shear due to transformation on fracture in notched PSZ specimens subjected to cyclic compression [12]. Despite deviations in crack path, the effectiveness of pre-cracking in cyclic compression is evident from the straight macroscopically Mode I tensile crack propagated subsequently in these specimens.

4. A model for the growth of short cracks in transforming ceramics

The present work has shown that under cyclic loading conditions, subcritical crack growth can occur at stress intensity values far below the fracture toughness generally considered appropriate for transformation-toughened ceramics. While this observation is consistent with the results of recent studies [21, 23], our investigation reveals several new features and mechanisms of fatigue crack growth in the zirconia ceramic. Two major trends evident from our new results are as follows: (i) Growth of short cracks under cyclic tension in Mg-PSZ is highly discontinuous in nature. Cracks tend to arrest naturally after some stable growth. Reinitiation of fracture cannot be achieved without an increase in the far-field stress intensity. (ii) Short crack growth under cyclic tension appears to be governed by a mechanism where the microscopic fracture events are similar to static/quasi-static fracture conditions. The major difference between quasi-static and fatigue fracture seems to be a consequence of the enhanced closure effects of the transformed wake during constant amplitude cyclic loading.

4.1. Conditions determining the range of crack growth

The results of our study lead us to formulate the following model which rationalizes the experimentally observed tensile fatigue crack growth in partially stabilized zirconia.

(i) The threshold stress intensity range, ΔK_0, for crack growth is reached when the maximum nominal stress intensity factor of the fatigue cycle, $K_{I\max}$, is

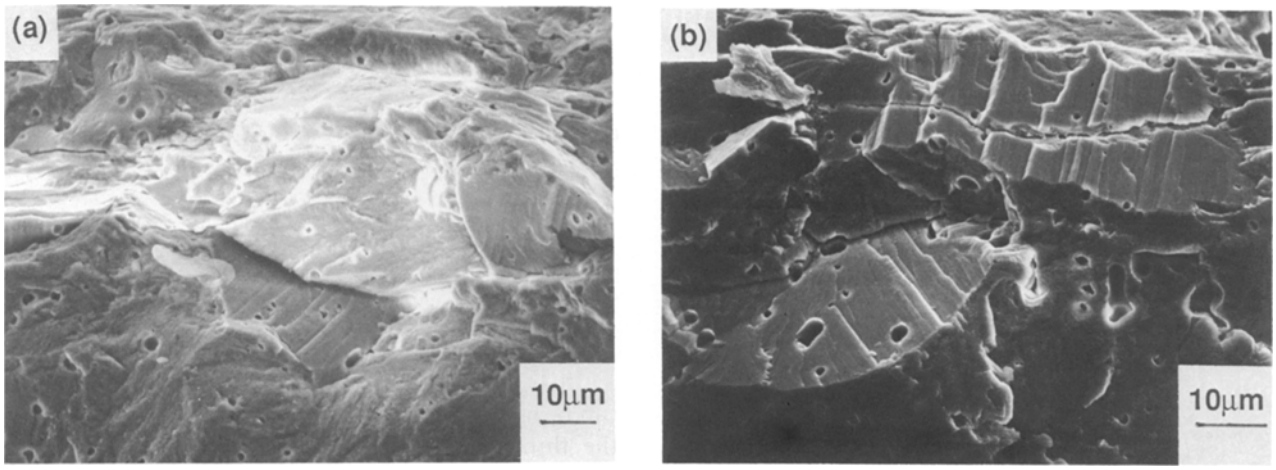

Figure 5 Fracture morphology during crack advance under far-field cyclic compression in two different specimens of Mg-PSZ.

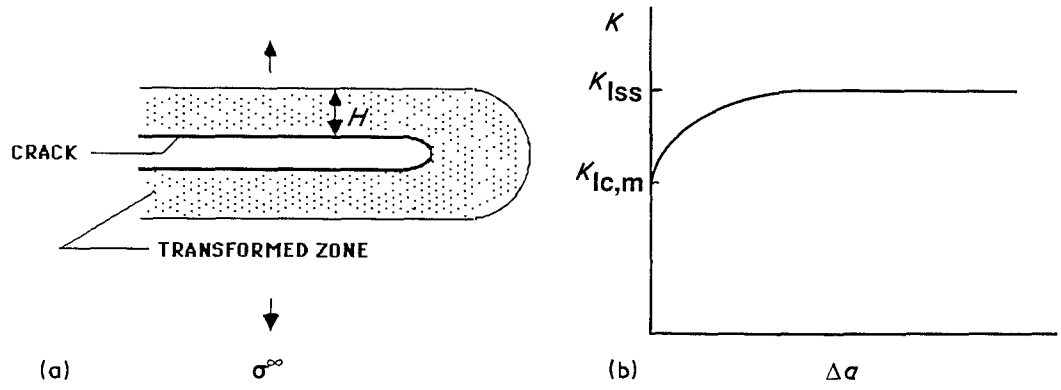

Figure 6 A schematic diagram of (a) the transformed wake during steady state crack growth; and (b) the resistance curve resulting from transformation at the crack-tip.

equal to the fracture toughness of the fully stable cubic zirconia matrix material, $K_{Ic,m}$.

$$\Delta K \rightarrow \Delta K_0 \text{ when } K_{Imax} = \frac{\Delta K}{(1-R)} \rightarrow K_{Ic,m} \quad (3)$$

(ii) Once crack growth is initiated, fracture occurs at a rapid rate over a distance, Δa^*, which is several times the width of the transformed zone, H (see Fig. 6). As the transformed material is moved to the wake of the advancing crack front, crack closure develops. Consequently, the effective driving force for tensile fatigue fracture, ΔK_{eff}, has a much smaller value than the nominal (far field) ΔK for constant amplitude of tensile loading at a fixed R.

$$\Delta K_{eff} = \Delta K - \Delta K_{cl} \quad (4)$$

This effect results in complete crack arrest, and further crack advance can be easily resumed with an increase in the far-field stress intensity.

(iii) Catastrophic fracture occurs at $\Delta K = \Delta K_f$ when the maximum stress intensity factor of the fatigue cycle approaches the steady state toughness value, K_{Iss} (see the R-curve in Fig. 6b) of the partially stabilized zirconia; i.e. when

$$K_{max} = \frac{\Delta K_f}{(1-R)} \rightarrow K_{Iss} \quad (5)$$

Theoretical analyses of the effect of stress-induced dilatant transformations during quasi-static tensile fracture on crack closure ("shielding") levels in zirconia have recently been reported [17–19]. Such analyses predict the extent of toughening to be (e.g. [18])

$$K_{Iss} - K_{eff} \approx 0.2143 \frac{EV_f e^T}{(1-\nu)} H^{1/2} \quad (6)$$

where E is Young's modulus, V_f the volume fraction of the transforming particles, e^T the transformation strain, and ν Poisson's ratio. The distance over which the shielding effect due to transformation is maximized is [17]

$$\Delta a^* \approx 5H \quad (7)$$

4.2. Width of transformed zone and extent of stable crack growth

In order to evaluate the validity of the above arguments, currently available experimental measurements of the size of the transformed zone are now examined in conjunction with the fatigue test results. Three sets of data, which have been reported in the literature [25–27], are summarized below.

(i) The measurements of Porter and Heuer [25] and Schoenlein [26] on 8.5 mol % MgO-PSZ show that $H = 0.6\,\mu m$, $V_f = 0.3$, $E = 200\,GPa$, and $e^T = 0.058$. Based on these results, one would predict a value of $\Delta a^* \approx 3\,\mu m$ from Equation 7.

(ii) Budiansky *et al.* [18] quote the unpublished work of Swain who studied the transformation process in two-phase Mg-PSZ where the estimates are as follows: $H \approx 1\,\mu m$, $V_f = 0.3$, $E = 170\,GPa$, and $e^T = 0.04$. From this, one obtains $\Delta a^* \approx 5\,\mu m$.

(iii) Claussen and Ruhle [27] studied the transformation of zirconia particles in an alumina matrix where they found that $H \approx 5\,\mu m$ with $E = 470\,GPa$, $V_f = 0.3$, and $\theta^T = 0.04$. From this, one obtains $\Delta a^* \approx 25\,\mu m$.

Table I summarizes the experimentally measured values of Δa^* at different ΔK levels corresponding to the tensile fatigue results of Fig. 2. A comparison of Table I with the above calculations (i) to (iii) for Δa^* suggests that the distance of growth necessary to build up the maximum crack-tip shielding effect (closure) in each increment of fatigue crack growth is of the same order of magnitude as the Δa^* value for maximum toughening predicted by the purely dilatational transformation theories [17, 18].

The maximum enhancement in toughness predicted by Equation 6 for stress-induced dilatant transformation, K_{Iss}–K_{eff}, is 0.73, 0.94 and 2.1 MPa $m^{1/2}$ for H = 0.61, 1 and 5 μm, respectively, with $E = 205\,GPa$. $\nu = 0.3$, $V_f = 0.3$, and $e^T \approx 0.5$ for Mg-PSZ. In the context of crack growth under cyclic tension, the shielding effect of transformation, $\Delta K_{cl} = 0.73$ to 21 MPa $m^{1/2}$ would be sufficient to completely arrest the crack during each increment of crack advance. For example, when crack growth occurs over a distance of about 37 μm at the threshold $\Delta K_0 \approx 3.45$ MPa $m^{1/2}$ (Table I), a reduced effective ΔK

$$\Delta K_{eff} = \Delta K - \Delta K_{cl} \quad (8)$$

can bring the near-tip stress intensity to a value below the threshold for crack growth. This reduction in ΔK triggers crack arrest. When the far-field ΔK value is raised to reinitiate the arrested crack, a larger

transformation zone is created at the crack-tip (as well as a larger crack opening displacement due to the higher ΔK). When this newly transformed zone is translated to the wake of the advancing crack front, the closure stress intensity range, ΔK_{cl}, is increased, thereby causing the crack to arrest. More recent measurements of the height of the transformed zone using Raman spectroscopy indicate that H can be as large as 100 m at high far-field K_I in PSZ [28]. This would imply a very dominant closure value ΔK_{Cl} for the present tests. It is not clear from the experiments or from the theory of dilatant transformation as to how the size of the transformed zone and the extent of closure continuously change with a varying far-field stress intensity during crack growth.

Note that martensitic transformation in partially stabilized zirconia is characterized by both volumetric and shear strains. It is now realized that estimates of the extent of crack-tip shielding based on the dilatational part of the transformation alone may severely underestimate the overall improvement in fracture resistance [17, 18]. Recently, numerical and analytical formulations have been reported where the contributions to compression fracture from both dilation and shear strains accompanying transformation have been incorporated in the constitutive models [12, 20]. Further work on the extension of these models to tensile fracture is necessary before the overall effects of transformation can be thoroughly analysed in the context of tensile fatigue.

The results of this work provide a clear experimental verification of the beneficial effect of shielding through observations of crack arrest. Although the occurrence of crack closure is directly confirmed by the documentation of crack arrest during cyclic tensile fracture, no direct closure measurements were made in this study. As significant fluctuations in the level of closure are observed over a very short distance of crack advance (between the crack initiation and crack arrest), global measurements of the closure stress do not, in this case, seem to provide a sufficiently accurate description of the changes in effective ΔK.

4.3. Comparison with experiments

The model proposed in this work for the conditions of stable tensile fatigue in transforming ceramics is consistent with a wide range of experimental observations.

(i) The microscopic models of fracture, as observed on the scanning electron micrographs, are similar for both quasi-static and cyclic tensile fracture. This phenomenon points to the possibility of "static modes" of failure during tension fatigue.

(ii) The range of K_{max} (at fixed R), over which stable crack growth occurs during constant amplitude tensile fatigue, coincides with the range of K values, over which stable quasi-static tensile fracture (R-curve) behaviour is observed in Mg-PSZ ([17–19] and Section 3 of this paper).

(iii) Theoretical analyses for transformation toughening predict a significant drop in the "effective driving force" for crack advance (at a fixed value of far-field tensile stress) after a certain distance of stable fracture, Δa^*. Direct observations of crack arrest, reported in this work, and measurements of crack closure, recently reported elsewhere [23], support these predictions. Furthermore, as demonstrated in the previous section, the experimentally measured values of Δa^* are comparable to the distance of crack advance over which the full beneficial effect of crack shielding by martensitic transformations is accomplished.

(iv) The fatigue specimens subjected to a static tensile load (by interrupting the fatigue test) show stable crack growth followed by crack arrest. This result provides additional supporting evidence to the implications of the model.

(v) It has been observed that an increase in the load ratio, R, leads to a reduction in the threshold ΔK_0 value [23]. However, according to Equation 3, the onset of crack growth at threshold appears to be controlled by the attainment of a fixed K_{max}.

(vi) In the frequency range 1 to 50 Hz, the maximum variation in growth rates observed in Mg-PSZ is less than a factor of 4, whereas stable crack growth is observed over growth rates spanning six orders of magnitude [23]. In view of the normal experimental scatter inherent in the *in situ* detection of crack velocity in ceramics, one may conclude that fatigue crack growth is essentially frequency-independent in the range 1 to 50 Hz. This behaviour is to be expected if tensile fatigue mechanisms are governed by static failure modes.

It is noted here that the threshold for fatigue crack growth, the microscopic failure mechanisms, the possibility of crack closure, and the similarities in the modes of failure between cyclic and quasi-static tension observed in this work on MS grade, Mg-PSZ are consistent with another recent work also on Mg-PSZ [23]. However, the characteristics of crack growth and the discontinuous nature of apparent tension fatigue (marked by periodic crack arrest) consistently found in the numerous experiments of this work have not been identified by Dauskardt *et al.* [23]. While the present study has examined the tensile fatigue behaviour of short flaws under predominantly plane strain conditions, longer cracks in thin specimens with a high degree of plane stress loading were investigated in [23]. The heat-treatment condition of the partially stabilized zirconia may have been different; the type of ageing condition was not clearly stated in [23]. The specimen geometry and crack detection method employed were also different in the two cases. The results reported in [23] on the effects of load ratio and frequency on crack growth, fractography, and closure are consistent with the model presented in this work. Although it has been suggested that transforming ceramics undergo intrinsic mechanical fatigue failure in cyclic tension [23], our results on short fatigue cracks appear to indicate that the apparent tensile fatigue crack growth response of transforming ceramics may be a direct manifestation of "static modes" of failure in the near-tip region.

It should, however, be noted that, despite their brittle fracture behaviour, all types of ceramics show stable crack growth under far-field cyclic compression which can be classified as a mechanical fatigue effect because it occurs only during unloading from a

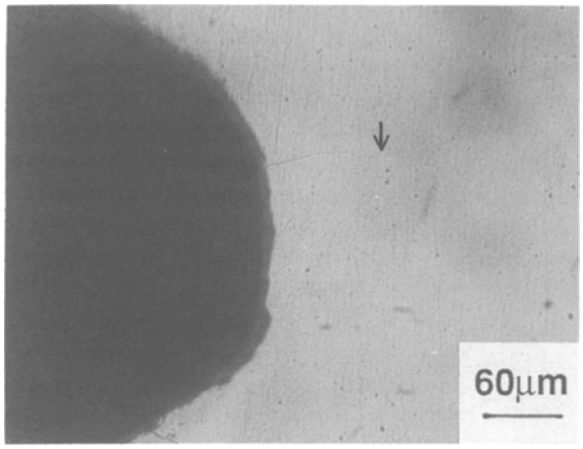

Figure 7 An optical micrograph showing a Mode I tensile fatigue crack in a tetragonal zirconia polycrystal partially stabilized with 2.5 mol % Y_2O_3 (Y-TZP). The arrow indicated the crack-tip location.

compressive stress and is completely different from the mode of failure observed under static, quasi-static, or environmentally assisted fracture [7–13]. Here residual tensile stresses generated during removal of the load induce a static-type of fracture. However, cycling of the far-field compressive stress is necessary to propagate the Mode I crack in this case.

5. Tensile fatigue crack growth in Y_2O_3-TZP

In addition to the results obtained in this work on tensile fatigue in Mg-PSZ, experiments were conducted to examine the possibility of crack advance under cyclic tension in tetragonal zirconia polycrystals partially stabilized with 2.5 mol % Y_2O_3. (Note that we have recently reported stable Mode I fatigue crack growth in notched plates of Y-TZP subjected to fully compressive far-field cyclic loads at room temperature; the details can be found in the Appendix of [8].) The microstructure of this material contains a random mixture of stable cubic and metastable tetragonal grains of average diameter about 0.4 to 0.7 μm. Fig. 7 shows an example of a Mode I fatigue crack propagated in a notched four-point bend specimen (without a fatigue pre-crack) subjected to cyclic tension at

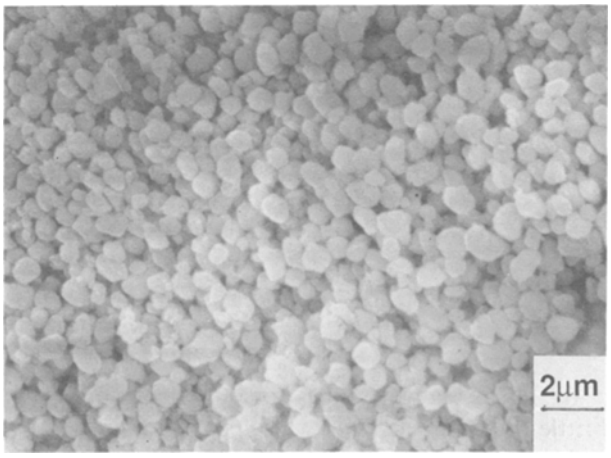

Figure 8 Fractography of tensile fatigue fracture in Y-TZP showing predominantly intergranular fracture.

$\Delta K \approx 4$ MPa $m^{1/2}$ and $R = 0.1$ in the room-temperature laboratory environment. In this case also, the range of stable fatigue fracture was observed at K_{max} values in between the toughness value of fully stabilized zirconia (about 3 MPa $m^{1/2}$) and the K_{Iss} for Y-TZP (about 6 MPa $m^{1/2}$). The fracture mode of Y-TZP in both quasi-static tension and cyclic tension was intergranular. Fig. 8 shows an example of the intercrystalline separation mode during tensile fatigue. These results for Y-TZP are in concurrence with the mechanisms proposed in the previous section for stable crack growth in transforming ceramics under cyclic tension.

6. Conclusion

The information presented in this paper clearly documents the possibility of stable crack growth under cyclic tension in transformation toughened ceramics. The basic features of short crack growth under cyclic tensile loads, however, are similar to those observed under quasi-static or static tensile loads. Furthermore, the interpretations derived from fractography, and from the effects of load ratio and frequency on crack growth in cyclic tension, tend to suggest that any apparent mechanical tensile fatigue effect observed in transforming ceramics may be a manifestation of the stable crack growth observed under static/quasi-static loads due to the shielding effect of the transformed crack-tip zone. The term "transformation plasticity" has recently been used to describe apparent toughening effects arising from martensitic transformations in ceramics, primarily as a result of the pronounced nonlinearity exhibited by the stress-strain curves for these materials [20]. However, the microscopic modes of failure in the transforming ceramics are still "brittle" as in the case of single-phase ceramics, except that they exhibit "apparently enhanced toughness" and "ductility" as a consequence of the transformation. Their microscopic mechanisms of stable crack growth are still vastly different from those observed in ductile solids, where dislocation motion (slip and damage accumulation in the plastically deformed near-tip region may contribute to progressive microfracture. In this context, the tensile fatigue results and model presented in this paper are consistent with the overall failure modes exhibited by the transforming ceramics. The information on crack arrest reported in Fig. 2 and Table I during tensile fatigue and static test also provides the most direct experimental verification of the significant shielding effect of crack tip transformation. Although this paper describes several key features of fracture in partially-stabilized zirconia under cyclic tension, considerable further work is necessary to elucidate and quantify the effects of mechanical variables (such as load ratio, frequency, wave form), microstructural variables (such as grain size, degree of stability, role of glassy phase, microcracking at the particle–matrix interface), and environmental variables (such as aqueous media, test temperature) on fracture under cyclic tension. The present work, in conjunction with available information, indicates that the growth of tensile fatigue cracks in ceramics is strongly affected by crack length

and shape, specimen geometry, loading method and stress state.

Acknowledgements

This work was supported by a National Science Foundation Grant NSF-ENG-8451092. Thanks are due to Mr J. Brockenbrough for helpful discussions and to Ms Karen Martino for typing the manuscript.

References

1. "Transfromation Toughening", Special Issue of *J. Amer. Ceram. Soc.* **66** (3) (1986).
2. D. A. KROHN and D. P. H. HASSELMAN, *J. Amer. Ceram. Soc.* **55** (1972) 208.
3. F. GUIU, *J. Mater. Sci.* **13** (1978) 1357.
4. A. G. EVANS and M. LINZER, *Int. J. Fract.* **12** (1976) 217.
5. A. G. EVANS and E. R. FULLER, *Metall. Trans.* **5A** (1974) 27.
6. A. G. EVANS, *Inter. J. Fract.* **16** (1980) 485.
7. L. EWART and S. SURESH, *J. Mater Sic. Lett.* **5** (1986) 774.
8. *Idem, J. Mater. Soc.* **22** (1987) 1173.
9. S. SURESH, *Engng Fract. Mech.* **21** (1985) 453.
10. S. SURESH and L. A. SYLVA, *Mater. Sci. Engng* **83** (1986) L7.
11. J. R. BROCKENBROUGH and S. SURESH, *J. Mech. Phys. Solids* **35** (1987) 721.
12. S. SURESH and J. R. BROCKENBROUGH, *Acta Metall.* **36** (1988) in press.
13. S. SURESH, L. EWART, M. MADEN, W. SLAUGHTER and M. NGUYEN, *J. Mater. Sci.* **22** (1987) 1271.
14. A. G. EVANS and R. M. CANNON, *Acta. Metall.* **34** (1986).
15. M. V. SWAIN, "R-Curve Behaviour of Mg-PSZ and Its significance to Thermal Shock", NILCRA Ceramics, St Charles, Illinois (1986).
16. D. B. MARSHALL, *J. Amer. Ceram. Soc.* **66** (1986) 173.
17. R. M. McMEEKING and A. G. EVANS, *ibid.* **65** (1982) 242.
18. B. BUDIANSKY, J. W. HUTCHINSON and J. C. LAMBROPOULOS, *Int. J. Solids Struct.* **19** (1983) 337.
19. J. C. LAMBROPOULOS, *Int. J. Solids Struct.* **22** (1986).
20. I.-W. CHEN and P. E. REYERS-MORAL, *J. Amer. Ceram. Soc.* **65** (1982) 242.
21. M. V. SWAIN and V. ZELIZKO, "Rotating Bending Fatigue of Mg-PSZ", CSIRO report, Available as NILCRA Report, Nilcra Ceramics, St Charles Illinois (1986).
22. K. BOWEN, P. E. REYERS-MORAL and I. W. CHEN, in Proceedings MRS Symposium on Advanced Ceramics, Boston, December 1986, edited by P. F. Becker and M. V. Swain (The Materials Research Society, Boston, 1988) in press.
23. R. H. DAUSKARDT, W. YU and R. O. RITCHIE, *Commun. J. Amer. Ceram. Soc.* **70** (1987) C248.
24. K. P. L. KAVISHE, *Int. J. Fract.* **27** (1985) R13.
25. D. L. PORTER and A. H. HEUER, *J. Amer. Ceram. Soc.* **60** (1977) 1983.
26. L. SCHOENLEIN, MS thesis, Case Western Reserve University, Cleveland (1979).
27. N. CLAUSSEN and F. RUHLE, unpublished results, University of California, Santa Barbara (1986).
28. A. H. HEVEN, Research in progress, Case Western Reserve University, Cleveland (1988).

Received 27 July
and accepted 23 October 1987